J Biol Inorg Chem (2011) 16:961–972
DOI 10.1007/s00775-011-0796-5

ORIGINAL PAPER

Antidiabetic vanadium compound and membrane interfaces: interface-facilitated metal complex hydrolysis

Debbie C. Crans · Samantha Schoeberl · Ernestas Gaidamauskas · Bharat Baruah · Deborah A. Roess

Received: 14 March 2011 / Accepted: 9 May 2011 / Published online: 11 June 2011

Abstract The interactions of metabolites of the antidiabetic vanadium-containing drug bis(maltolato)oxovanadium(IV) (BMOV) with lipid interface model systems were investigated and the results were used to describe a potentially novel mechanism by which these compounds initiate membrane-receptor-mediated signal transduction. Specifically, spectroscopic studies probed the BMOV oxidation and hydrolysis product interaction with interfaces created from cetyltrimethylammonium bromide (CTAB) which mimics the positively charged head group on phosphatidylcholine. ^{1}H and ^{51}V NMR spectroscopies were used to determine the location of the dioxobis(maltolato)oxovanadate(V) and the maltol ligand in micelles and reverse micelles by measuring changes in the chemical shift, signal linewidth, and species distribution. Both micelles and reverse micelles interacted similarly with the complex and the ligand, suggesting that interaction is strong as anticipated by Coulombic attraction between the positively charged lipid head group and the negatively charged complex and deprotonated ligand. The nature of the model system was confirmed using dynamic light scattering studies and conductivity measurements. Interactions of the complex/ligand above and below the critical micelle concentration of micelle formation were different, with much stronger interactions when CTAB was in the form of a micelle. Both the complex and the ligand penetrated the lipid interface and were located near the charged head group. These studies demonstrate that a lipid-like interface affects the stability of the complex and raise the possibility that ligand exchange at the interface may be important for the mode of action for these systems. Combined, these studies support recently reported in vivo observations of BMOV penetration into 3T3-L1 adipocyte membranes and increased translocation of a glucose transporter to the plasma membrane.

Keywords Antidiabetic vanadium complex · Drug interactions at membrane interfaces · Cetyltrimethylammonium bromide · Cationic surfactant · Micelle

Abbreviations

BMOV	Bis(maltolato)oxovanadium(IV)
cmc	Critical micelle concentration
CTAB	Cetyltrimethylammonium bromide
DLS	Dynamic light scattering

Electronic supplementary material The online version of this article (doi:10.1007/s00775-011-0796-5) contains supplementary material, which is available to authorized users.

D. C. Crans (✉)
Department of Chemistry,
Colorado State University,
Fort Collins, CO 80523-1872, USA
e-mail: crans@lamar.colostate.edu

S. Schoeberl · D. A. Roess (✉)
Department of Biomedical Sciences,
Colorado State University, Fort Collins,
CO 80523-1680, USA
e-mail: daroess@lamar.colostate.edu

E. Gaidamauskas
Vilnius University Institute of Biochemistry,
Mokslininku 12,
08662 Vilnius, Lithuania

B. Baruah
Department of Chemistry and Biochemistry,
Kennesaw State University,
Kennesaw, GA 30144, USA

DSS	4,4-Dimethyl-4-silapentane-1-sulfonic acid sodium salt
RM	Reverse micelle
AOT	Sodium bis(2-ethylhexyl)sulfosuccinate (also abbreviated Aerosol-OT)
dipic	2,6-pyridinedicarboxylate
ma	maltolato

Introduction

Drug interactions with cell membranes can be critical for cell delivery and for the drug to reach the site of subsequent action. The mechanism of action of the antidiabetic vanadium-containing drug bis(maltolato)oxovanadium(IV) (BMOV; Fig. 1) [1–5] is generally attributed to inhibition of intracellular protein tyrosine phosphatases [6–9]. Recently, modes of action affecting signal transduction pathways and thus involving the membrane in an alternative manner have been proposed for this class of antidiabetic agents [10–18]. Uptake of BMOV by Caco-2 (human colon adenocarcinoma) cells [15] and by human erythrocytes [14] via simple passive diffusion was found to induce morphological changes in the microvilli [15] and to increase order in the erythrocyte membrane structure [14]. BMOV also enhanced signaling in rat basophilic leukemia cells (RBL-2 H3), possibly via the receptor translocation into plasma membrane microdomains [10]. A neutral complex, bis(allixinato)oxovanadium(IV), with a coordinating environment similar to that of BMOV was found to penetrate mouse fibroblast adipocyte (3T3-L1) and to increase the translocation of glucose transporter 4 on the plasma membrane [19]. Interactions between oxidized BMOV and a negatively charged interface and cell studies showed that these compounds affect membrane fluidity and initiation of signal transduction through plasma membrane receptors [10, 20, 21].

Cellular membranes are heterogeneous structures composed primarily of lipids and integral membrane proteins. Given the dynamic nature of the membrane, the diversity of proteins incorporated in and associated with the membrane, and the membrane heterogeneity, information on drug interactions with cellular membranes is difficult to obtain directly and often information is obtained indirectly using model systems. For such studies to be most effective, limitations of the model system should be recognized and considered. Various model systems have been used with success and permit study of various aspects of drug interactions with lipids. For example, vesicle systems offer the advantages of maintaining the parent lipid bilayer structure and study of a semistable system [22–26]. Monolayers allow examination of interactions at the water-lipid-interface layer and interactions between the drug and bulk and interface water. Langmuir monolayers [27], micelles [28–30], and reverse micelles (RMs) [31–36] (Fig. 1) represent three different interfaces. The micellar and

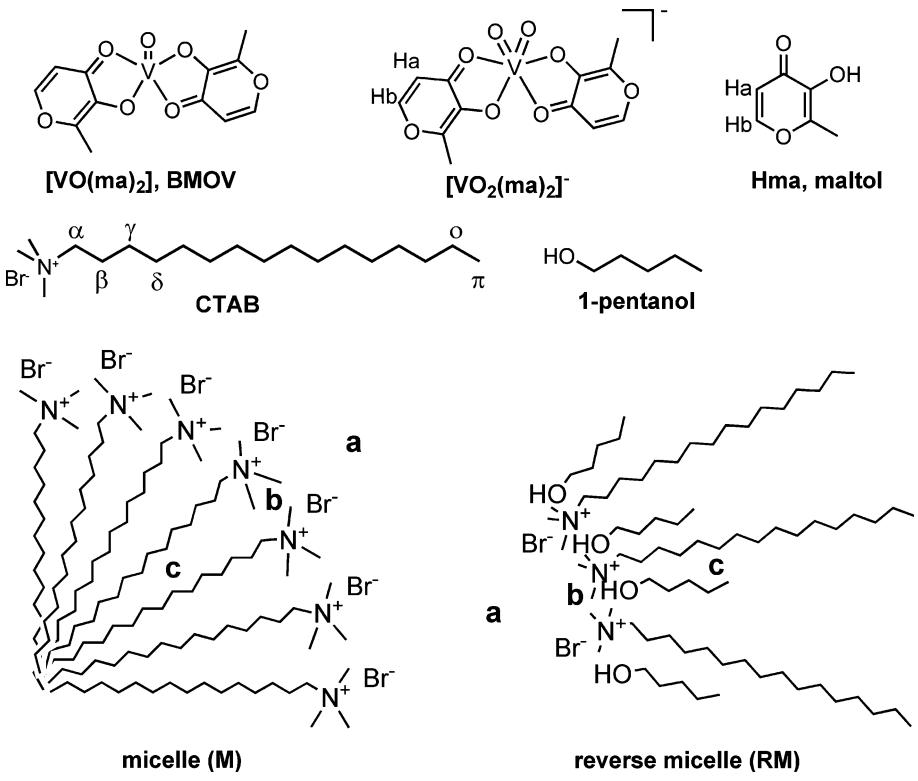

Fig. 1 Structures of the bis(maltolato)oxovanadium(IV) (*BMOV*) complex, the oxidized BMOV complex ($[VO_2(ma)_2]^-$), the maltol ligand (*Hma*), cetyltrimethylammonium bromide (*CTAB*), and 1-pentanol. Cross sections of a CTAB micelle (*M*) and a CTAB reverse micelle (*RM*) are shown with possible probe molecule locations in the water pool (*a*), on the polar interface (*b*), and in the nonpolar region of the surfactant (*c*)

reverse-micellar systems are the simplest models and can provide information on the location of a potential drug within the interface. Given the importance of Coloumbic interactions and the specific change-dependent effects, we seek to document the fundamental difference in interactions with the interface compared with simple charge interactions. Spectroscopic studies of the simple micellar and reverse-micellar systems provide details on how potential drugs may interact with cellular lipid interfaces.

Cetyltrimethylammonium bromide (CTAB), a positively charged surfactant, is an excellent model for the phosphatidylcholine head group and is used in many systems as a lipid substitute. At 1.0 mM, CTAB spontaneously forms spherical micelles that are approximately 5.8 nm in diameter and contain an average of 100 surfactant molecules. CTAB micelles can be characterized using dynamic light scattering (DLS), small angle neutron scattering, conductivity measurements, and NMR spectroscopy [37–40]. CTAB micelle interaction with spectroscopic probes has been studied by NMR [29, 30], EPR [41], fluorescence [42–44], and UV–vis [44, 45] spectroscopies. A number of studies with probe molecules have shown that in some cases a sphere-to-rod transition occurs [46–48], whereas in other cases there is little change in micellar shape [29]. Formation of RMs using CTAB generally requires the presence of a cosurfactant, a short-chain alcohol that facilitates self-assembly into spherical nanosized structures with approximately 5.0 nm diameter. The properties of RMs have also been characterized using a range of methods, such as DLS, conductivity measurements, quasielastic light scattering, near-infrared absorption spectroscopy, and pulsed field gradient spin–echo NMR spectroscopy [38–40], and a range of probes [29, 35]. Together these systems provide positive and negative surface curvature observed in the interior and exterior of biological membrane, although the degree of curvature in these systems is greater than in the cellular membrane.

The chemistry of vanadium complexes under physiological conditions is complex and sensitive to the environment of the compounds [2]. BMOV contains vanadium in oxidation state IV and is not stable under physiological conditions. Specifically, the complex will hydrolyze to form free ligand and metal ion as well as oxidize to form the V(V) complex $[VO_2(ma)_2]^-$ (where ma is maltol) as shown in Fig. 1. These conversions are likely to occur under physiological conditions [49, 50] as well as in biotransformations resulting from reactions with available ligands in vivo. To attribute observed effects to a specific vanadium complex, a series of studies are generally conducted to determine the effects of the decomposition products. To probe interactions with membranes, a simple system, in which different vanadium complexes can be studied, will be used.

Specifically, we have investigated how the oxidized metabolites of the antidiabetic drug BMOV, $[VO_2(ma)_2]^-$, and its ligand maltol interact with a positively charged lipid interface to evaluate how these molecules might interact with a cell membrane interface. Previous studies using NMR spectroscopy provided information on how deep potential drugs penetrate the interface [28–30, 36, 51]. Since BMOV contains V(IV), it is paramagnetic and cannot be examined using NMR spectroscopy [52]. In contrast, the oxidized complex and the maltol ligand can be readily examined using ^{51}V and ^{1}H NMR spectroscopies and information on their local environments can be obtained. The studies reported in this article describe the interactions of oxidized BMOV and maltol with both micelles and RMs with a phosphotidylcholine-like surface and demonstrate how readily these molecules penetrate the interface.

Materials and methods

All reagents except CTAB were used as received without further purification: anhydrous $NaVO_3$ (99.9%, Aldrich), maltol (99%, Aldrich), D_2O (Cambridge Isotope Laboratories), sodium deuteroxide (30 wt%, 99+ at%, Aldrich), deuterium chloride (35 wt%, 99 at%, Aldrich), cyclohexane (high performance liquid chromatography grade, Fisher Scientific), and 1-pentanol (99%, Aldrich). CTAB (99%, Sigma) was recrystallized from anhydrous ethanol and dried overnight under a vacuum over anhydrous calcium sulfate [40].

Stock solution of $Na[VO_2(ma)_2]$ and maltol

The $[VO_2(ma)_2]^-$ complex was prepared from $NaVO_3$ and maltol in solution as described previously [53]. A 100 mM stock solution of $Na[VO_2(ma)_2]$ was prepared by adding 2.5 mL of 200 mM $NaVO_3$ to the solid maltol (0.126 g, 1.0 mmol) in a 5-mL volumetric flask. The solution was stirred with gentle warming to completely dissolve the solid. The solution pH was adjusted as needed and the solution was diluted to the final volume. The light-yellow appearance of these solutions is distinctly different from the intense yellow color observed for decavanadate-containing solutions and the spectroscopic characteristics of the solution were as reported previously [53]. The pH of solutions was measured using a Thermo Scientific Orion 2-Star pH meter equipped with a combined semi-micro pH electrode (VWR, 14002-766).

Micellar sample preparation

A 200 mM stock solution of CTAB was prepared by dissolving purified CTAB in deionized water and warming the mixture until the solution was clear. All samples for ^{1}H and ^{51}V NMR spectroscopies were prepared by combining

$[VO_2(ma)_2]^-$, maltol, and CTAB stock solution, followed by incubation at 35 °C. Turbid solutions obtained with 2.0 mM $[VO_2(ma)_2]^-$ and CTAB in the concentration range from 1 to 10 mM were not used for NMR spectroscopy. The spectra shown here are only for transparent solutions with no precipitate.

Reverse-micellar sample preparation

Preparation of a representative 1-mL sample of a RM ($w_0 = [H_2O]/[CTAB] = 4$) is described. To solid CTAB (36.4 mg, 0.10 mmol), 1-pentanol (54.3 μL, 0.50 mmol) was added to obtain a 5:1 ratio of cosurfactant to surfactant [54, 55]. Next, 938 μL of cyclohexane was added, followed by 7.2 μL of aqueous stock of 0.100 M $[VO_2(ma)_2]^-$ or 0.200 M maltol. The mixture was vortexed for a few seconds until the solution was clear. Various w_0 values were obtained by varying the volumes of cyclohexane and aqueous stock solution. All samples used for NMR spectroscopy were clear, transparent solutions.

Conductivity

Conductivity was used to characterize CTAB micelle formation. Solutions with various concentrations of CTAB alone and CTAB containing 2.0 mM $Na[VO_2(ma)_2]$ were prepared. Solution conductivity was measured with a Thermo Orion 150 A+ conductivity meter equipped with a platinum conductivity cell (Thermo Orion, 011020) in at 35 °C thermostated vial, above the CTAB Krafft temperature (26 ± 1 °C) [56, 66].

Dynamic light scattering

DLS (Wyatt DynaPro Titan) measurements were made of both the micellar and reverse-micellar samples. Prior to data acquisition, samples were equilibrated in the DLS instrument for 10 min at 35 °C. Each measurement consisted of at least ten runs, each of which used a set number of scans. Scans were performed at a rate of ten acquisitions per 100 s.

^{1}H NMR spectroscopy of micelles and RMs

A Varian Inova 400 NMR spectrometer operating at 400.107 MHz was utilized to obtain ^{1}H NMR spectra at about 22 °C of CTAB reverse-micellar samples as reported previously [30]. Spectra of the CTAB micellar samples were acquired using a Varian Inova 300 spectrometer operating at 299.953 MHz at constant 35 °C. Samples were allowed to equilibrate for approximately 10 min prior to acquisition.

Because of the importance of referencing in these studies and the complexity of some of the samples, extensive work has been undertaken to improve our procedures and comparisons of aqueous and organic samples (Crans DC, Bonetti S, Woll KA, Trujillo AM, Schoeberl S, Gaidamauskas E, Christakos J, Johnson MD et al., unpublished work). Both external and internal referencing recommended by IUPAC [57] were routinely used. Aqueous samples are generally referenced against internal or external 4,4-dimethyl-4-silapentane-1-sulfonic acid sodium salt (DSS; $\delta = 0.000$ ppm) in D_2O. Aqueous (for comparison with micellar and reverse-micellar samples) and aqueous micellar samples were referenced against internal DSS ($\delta = 0.000$ ppm) in D_2O, external DSS in D_2O, or an external sample of tetramethylsilane ($\delta = 0.000$ ppm) in benzene-d_6 placed in a coaxial capillary with a frequency lock. Generally, the chemical shifts in the aqueous phase were the same within ±0.002 ppm. We used the benzene-d_6 peak at 7.157 ppm as an additional reference for aromatic protons of the probe [29, 30]. Data on the reverse-micellar samples were acquired without a frequency lock and the samples were referenced internally against the cyclohexane-H_{12} signal at 1.443 ppm. This chemical shift was determined for C_6H_{12} in cyclohexane-d_{12} with internal tetramethylsilane ($\delta = 0.000$ ppm), and was different from the cyclohexane-d_{11} residual peak at 1.382 ppm.

^{51}V NMR spectroscopy of micelles and RMs

The ^{51}V NMR spectra were recorded using a broadband Varian Inova 300 spectrometer operating at 78.9 MHz using acquisition parameters as described previously [20]. A $VOCl_3$ standard ($\delta = 0.00$ ppm) was used for chemical shift referencing.

Results and discussion

Interaction of $[VO_2(ma)_2]^-$ with CTAB micelles

^{1}H and ^{51}V NMR spectroscopies are powerful tools to probe the location of a $[VO_2(ma)_2]^-$ complex in lipid interfaces and complex stability. The hypothesis that $[VO_2(ma)_2]^-$ is interacting with the CTAB micellar interface was examined utilizing NMR spectroscopy. CTAB forms micelles in aqueous solution above the Krafft temperature of 26 ± 1 °C [56] and above the critical micelle concentration (cmc) of approximately 1 mM [58]. Below this value, CTAB exists in its monomeric and premicellar form that is distributed in aqueous solution. We investigated this complex in CTAB micelles prepared using aqueous solutions of $[VO_2(ma)_2]^-$ with pH values of 7.4, 8.2, and 9.1. As shown in Fig. 2, no change was observed in ^{1}H NMR chemical shifts of $[VO_2(ma)_2]^-$ in CTAB micelles at the different pH values. In aqueous solution without CTAB, most of the

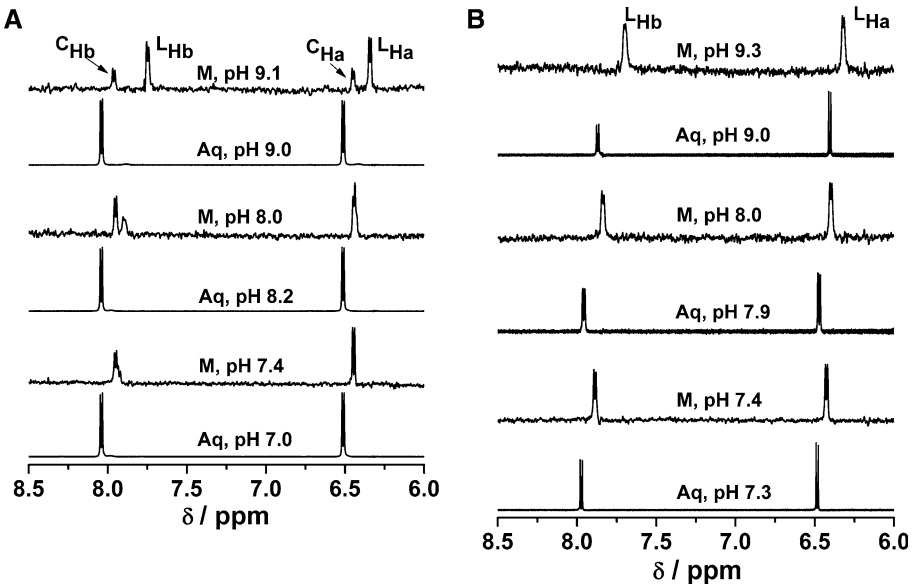

Fig. 2 The ^{1}H NMR spectra of 2 mM $[VO_2(ma)_2]^-$ (**a**) and 4 mM maltol (**b**) as a function of pH in D_2O aqueous solutions and in 50 mM CTAB micellar samples. The Ha and Hb protons are labeled as C_{Ha} and C_{Hb} for the $[VO_2(ma)_2]^-$ complex and as L_{Ha} and L_{Hb} for the maltol ligand. Spectra were recorded at 35 °C. The pH values shown were not corrected for the presence of D_2O

$[VO_2(ma)_2]^-$ remains intact and the amounts do not change from pH 7 to 9 [53]. However, in the CTAB micellar solution, both C_{Ha} and C_{Hb} protons shift upfield, indicating complex penetration into a nonpolar micellar environment. Additionally, the complex decomposes according to the reaction shown in Eq. 1, and the extent of decomposition increases with solution pH. In the 2.0 mM $[VO_2(ma)_2]^-$ solution, about 90% of the complex remains intact at pH 7.4, at pH 8.0 66% of it is intact, and at pH 9.1 only 33% of the complex remains in solution.

We then investigated $[VO_2(ma)_2]^-$ complex stability at various concentrations of CTAB. Data are shown in Fig. 3 from ^{1}H NMR spectra of CTAB in solutions without a probe molecule and with 2.0 mM $[VO_2(ma)_2]^-$ probe. Chemicals shifts for the $C_\alpha H_2$ and $N(CH_3)_3$ protons in the CTAB molecule changed the most, suggesting that the $[VO_2(ma)_2]^-$ complex is interacting most with these protons in the micelle. The difference was only observed above CTAB concentrations when micelles forms. At high CTAB concentration, the difference becomes small because the probe-to-micelle ratio is too small to measure the effect.

$$\left[VO_2(ma)_2\right]^- + 2H_2O \rightleftharpoons H_2VO_4^- + 2\,Hma. \quad (1)$$

To confirm that observed effects are due to CTAB micelles and not individual CTA^+ and $[VO_2(ma)_2]^-$ ion interaction, we used ^{51}V NMR spectroscopy of $[VO_2(ma)_2]^-$ in aqueous solution and at differing CTAB concentrations (Fig. 4). Below the cmc of CTAB, the complex associated less with the CTAB, although less of the complex and some of the 1:1 complex ($[VO_2(ma)(OH)(H_2O)]^-$) were observed in these solutions. This conclusion is based on the modest if any line broadening of the complex signal observed at concentrations below the cmc (below 1 mM CTAB).

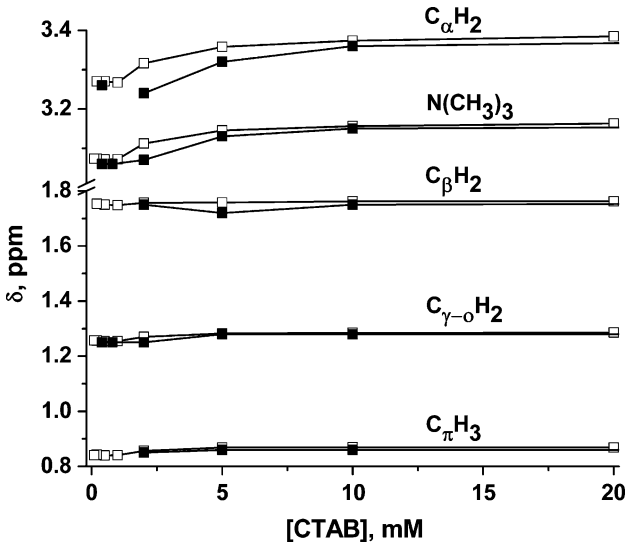

Fig. 3 The ^{1}H chemical shifts of CTAB signals as a function of CTAB concentration in solution with the $[VO_2(ma)_2]^-$ probe (*filled squares*) and without the probe (*open squares*) at pH 9.0 in H_2O. Spectra were recorded at 35 °C with the lock on benzene-d_6 in a coaxial capillary. Chemical shifts are referenced against the tetramethylsilane (0.00 ppm) added to benzene-d_6

At CTAB concentrations above the cmc, the $[VO_2(ma)_2]^-$ complex was found to associate with micelles, as evidenced from the line broadening observed in solutions prepared with 10 mM CTAB or higher CTAB concentrations. These results are consistent with those shown in Fig. 2 and again suggest the partial penetration or association of $[VO_2(ma)_2]^-$ with the micellar interface.

The ^{51}V NMR data also confirm that the $[VO_2(ma)_2]^-$ complex decomposes into free vanadate(V) species, with monomer V_1 (at −559 ppm) as the predominant species

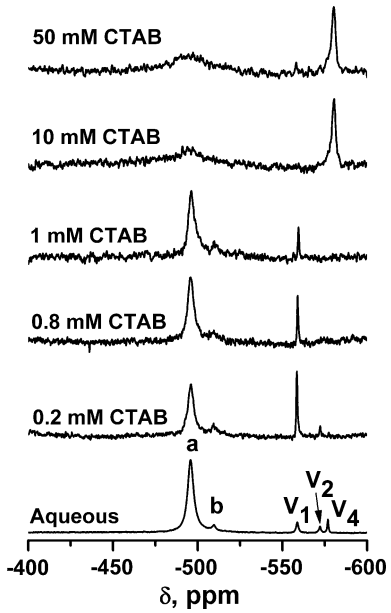

Fig. 4 ^{51}V NMR spectra of 2.0 mM $[VO_2(ma)_2]^-$ in aqueous solution and 50 mM CTAB solutions at pH 7.3. The CTAB concentration is shown next to each spectrum. The resonances shown are $[VO_2(ma)_2]^-$ (*a*), $[VO_2(ma)(OH)(H_2O)]^-$ (*b*), $H_2VO_4^-$ (V_1), $H_2V_2O_7^{2-}$ (V_2), and $V_4O_{12}^{4-}$ (V_4)

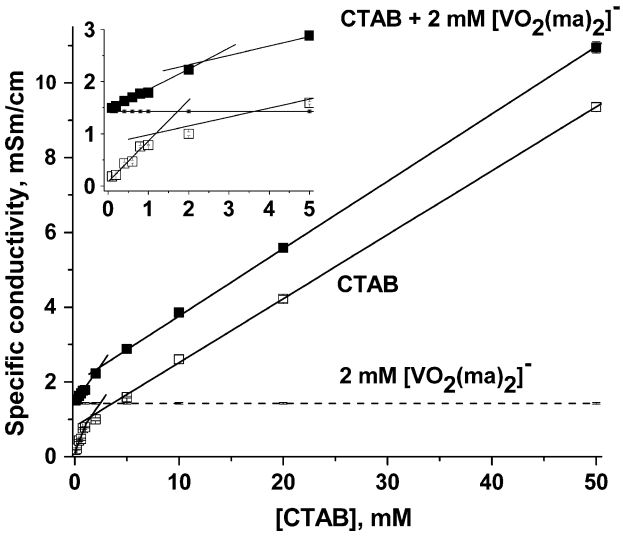

Fig. 5 Specific conductivity at 35 °C of aqueous CTAB with 2.0 mM $[VO_2(ma)_2]^-$ (*filled squares*) and CTAB without the probe (*open squares*) as a function of CTAB concentration. The specific conductivity of the aqueous 2.0 mM $[VO_2(ma)_2]^-$ is shown as the *dashed line*. The pH of all samples was 7.3 ± 0.2. *Error bars* represent three standard deviations of five replicates and, if not visible, are small and covered by the symbol. The *inset* shows the break in specific conductivity below and above the critical micelle concentration of CTAB

below the cmc, and tetramer V_4 as the predominant species above the cmc. Vanadium(V) speciation equilibria show that V_1 is the major species at low concentrations and low ionic strength and higher oligomers are the major species at higher concentrations and high ionic strength [59–61]. Although higher oligomers generally are accompanied by some V_1, the small amounts of higher oxovanadates below the cmc suggests that interactions of $[VO_2(ma)_2]^-$ with disperse CTAB molecules only shift the stability of the complex slightly. In contrast, interactions of $[VO_2(ma)_2]^-$ with the CTAB micelles significantly impact the formation constants because only one higher oxovanadate and no 1:1 complex is observed in addition to the $[VO_2(ma)_2]^-$ complex. The aqueous V_1, V_2, V_4, and V_5 species are in rapid equilibrium on the NMR timescale [2, 62], although this may not be observed under these conditions because the mobility has decreased. The significant line broadening observed for the oligomer signal (at −580.5 ppm assigned to V_5) could indicate that this species is strongly associating with a micellar interface as well as $[VO_2(ma)_2]^-$, possibly through electrostatic attraction. Alternatively, species associating with the micellar surface and in rapid equilibrium with oligomeric oxovanadates can produce similar line broadening [63, 64]. That both V_1 and V_2 are not observed in spectra above the cmc is unexpected. This suggests that V_1 and V_2 species may be associating with the interface as reported previously for RMs [64] and that this results in the broadening of higher oligomeric signals. Similar line broadening has been observed in cases where oligomeric oxovanadates were associating with a protein [34, 63, 65].

To confirm that the $[VO_2(ma)_2]^-$ complex does not alter the formation of CTAB micelles, we measured conductivity as a function of CTAB concentration in samples with and without 2.0 mM $[VO_2(ma)_2]^-$ at 35 °C, above the Krafft temperature of CTAB (26 ± 1 °C [66]). As shown in Fig. 5, $[VO_2(ma)_2]^-$ increased the conductivity of the micellar samples similarly below and above the cmc and that increase was approximately equal to the conductivity of 2.0 mM $[VO_2(ma)_2]^-$ solution. These results are consistent with one cmc and the formation of spherical micelles as reported previously [56, 58]. The appearance of only one cmc in CTAB solutions containing $[VO_2(ma)_2]^-$ that does not differ from the cmc of CTAB alone suggests that probe molecule does not significantly perturb the structure of CTAB micelles. There is precedence for both one and two cmc's in probe–surfactant systems [29, 67]. A second cmc appearing in systems with strong probe–surfactant interaction is generally indicative of the sphere-to-rod transition of micellar shape [46, 47].

Interaction of maltol with CTAB micelles

Since $[VO_2(ma)_2]^-$ hydrolyzes in the presence of micelles, it is important to investigate how the ligand, maltol, interacts with the micelle. Series of ^{1}H NMR spectra of 4.0 mM maltol in aqueous and CTAB micellar solutions

were acquired at pH values of 7.3/7.4, 7.9/8.0, and 9.0/9.3 (Fig. 2b). The ^{1}H NMR spectra show only a modest upfield chemical shift for the complex in the presence of micelles and below the pK_a of maltol. However, at pH 9.0/9.3 more upfield shifting was observed in micellar solutions as compared with aqueous solutions. Maltol deprotonates with increasing pH and the upfield ^{1}H NMR chemical shift is typical for most deprotonating molecules [68]. Since the maltol pK_a is 8.4 [69], part of the chemical shift in CTAB micelles with maltol must be attributed to deprotonation.

Because both penetration/association with the interface and deprotonation result in upfield shifts, studies performed above the pK_a value for maltol are important for examining penetration/association with the interface under conditions where little, if any, deprotonation is occurring. If the maltol ligand associates with or penetrates the micelle, then the CTAB protons should show the chemical shift changes accordingly. This possibility can be investigated by measuring the chemical shifts of CTAB above and below the cmc. As in the case of $[VO_2(ma)_2]^-$, the chemical shifts for most CTAB protons, with the exception of the alpha and $N(CH_3)_3$ protons, did not change (Table S1, spectra not shown). These observations suggest that the maltol ligand and the complex are located in similar parts of the micelle.

Interaction of $[VO_2(ma)_2]^-$ with CTAB/1-pentanol/cyclohexane/D_2O RMs

To complement studies with micelles, we explored the interaction of $[VO_2(ma)_2]^-$ with the cationic surfactant layer in RMs. These studies are done under complementary conditions because the aqueous solution is present as a small droplet within the organic solvent. The small amounts of water in these experiments explain the need for increased concentration of drug to obtain the needed sensitivity. Specifically, we used ^{1}H and ^{51}V NMR spectroscopies to characterize $[VO_2(ma)_2]^-$ interactions with RMs formed from CTAB/1-pentanol/cyclohexane. We were interested in determining whether the water pool size and the pH of the aqueous stock solution affected interface interactions between $[VO_2(ma)_2]^-$ and RMs of different sizes. These interactions were characterized at both neutral and basic pH, since the $[VO_2(ma)_2]^-$ complex is stable near neutral pH but hydrolyzes outside a narrow pH window. The ^{1}H NMR chemical shifts for the drug can be used to report its location, and thus provide information about the likely form of the compound near a biological interface.

In Fig. 6a the ^{1}H NMR spectra are shown for 100 mM $[VO_2(ma)_2]^-$ aqueous stock solution at pH 7.0 and in 0.20 M CTAB with 1.0 M 1-pentanol in cyclohexane. The w_0 ratio ranged from 4 to 20. As the water pool size decreased, resonances shifted upfield compared with aqueous solution with the exception of the methylene signals (spectra not shown), for which the chemical shifts were unchanged from those in aqueous stock solution. The upfield C_{Hb} and C_{Ha} signals were consistent with C_{Ha} that C_{Hb} being inside the hydrophobic environment of the reverse-micellar interface. Relatively small chemical shift changes for C_{CH_3} suggested that its location resembled that of an aqueous environment or that there were equal and opposite shifts induced by the nonpolar interface and the polar head groups (see Fig. 7a). Examples have been reported for each of these possibilities [20, 35, 36, 51, 70]. One interpretation of continuous upfield shifts with decreasing water pool size is that the metal complex is pushed into the nonpolar interface, most likely because the

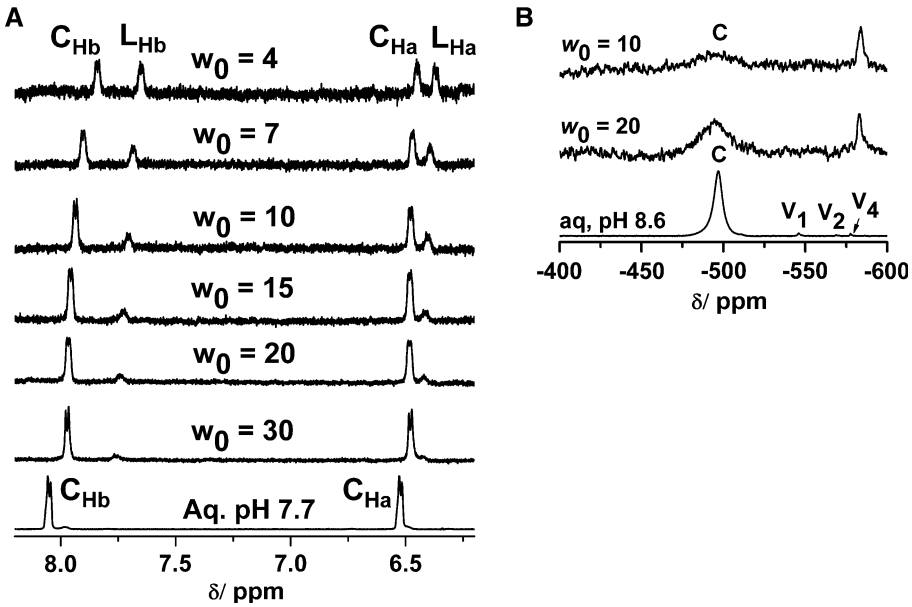

Fig. 6 **a** ^{1}H NMR spectra of $[VO_2(ma)_2]^-$ at pH 7 in aqueous stock solution and in CTAB reverse-micellar samples with differing w_0. CTAB reverse-micellar samples were prepared in 100 mM $[VO_2(ma)_2]^-$ and 0.2 M CTAB/1 M 1-pentanol/cyclohexane. **b** The ^{51}V NMR spectra of 100 mM $[VO_2(ma)_2]^-$ in D_2O at pH 8.6 and in CTAB reverse-micellar samples

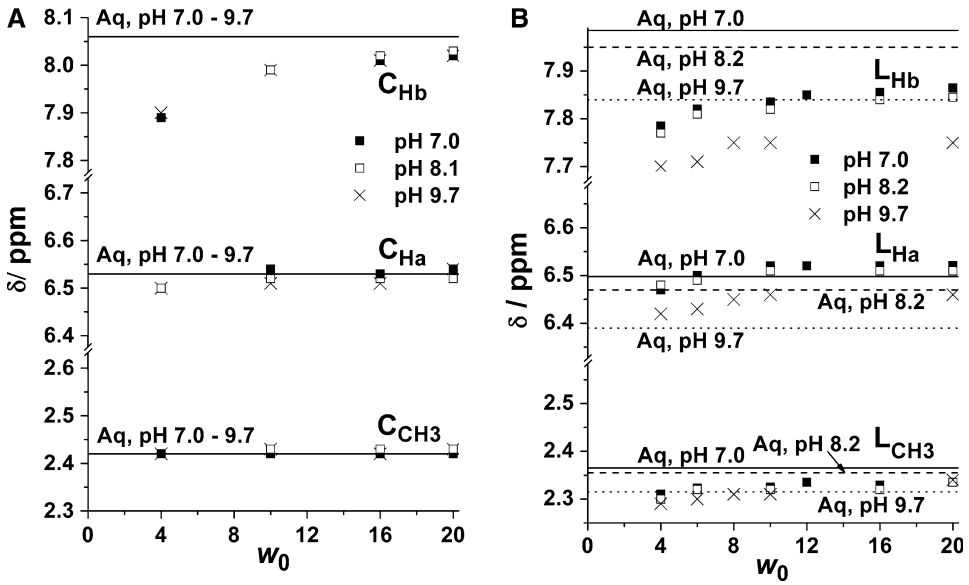

Fig. 7 The ^{1}H NMR chemical shifts of Ha, Hb, and CH_3 of the $[VO_2(ma)_2]^-$ complex (**a**) and the maltol ligand (**b**) in 0.2 M CTAB/1.0 M 1-pentanol/cyclohexane reverse micelles as a function of w_0 at pH 7.0 (*filled squares*), 8.2 (*open squares*), and 9.7 (*crosses*). The chemical shifts of the $[VO_2(ma)_2]^-$ complex are pH-independent and are shown as *solid lines*. The ^{1}H chemical shifts of maltol in aqueous stock solutions are shown at pH 7.0 (*solid lines*), 8.2 (*dashed lines*), and 9.7 (*dotted lines*). The pH-adjusted aqueous stock solutions of 100 mM $[VO_2(ma)_2]^-$ and 200 mM maltol were used to prepare reverse-micellar samples

water pool size approaches the molecular size of the complex. In addition, confinement in the small water pool of a RM had a profound effect on the stability of the complex; with decreasing w_0 (Fig. 6a), there was a dramatic increase in $[VO_2(ma)_2]^-$ decomposition into vanadate as reflected in the increase in the ratio between free ligand and complex (which is decreasing).

The $[VO_2(ma)_2]^-$ complex was also studied by ^{51}V NMR spectroscopy. Figure 6b shows spectra for 100 mM $[VO_2(ma)_2]^-$ aqueous stock solution and for $w_0 = 20$ and $w_0 = 10$ reverse-micellar solutions. The $[VO_2(ma)_2]^-$ resonance shifts downfield as w_0 decreases as was previously observed for $[VO_2(ma)_2]^-$ in AOT/isooctane [20]. Larger ^{51}V downfield shifts have been reported for V_{10} in AOT/isooctane [70] and for $[VO_2(dipic)]^-$ in CTAB/*n*-pentanol/cyclohexane [35] in RMs. The spectra shown in Fig. 6b differ from those for $[VO_2(dipic)]^-$ in CTAB/pentanol/cyclohexane RMs, where was no change as w_0 decreased and the linewidth was constant for all samples [35]. Since no ^{51}V NMR chemical shift differences were observed with $[VO_2(dipic)]^-$ in AOT/isooctane [36] and there is a change for the $[VO_2(ma)_2]^-$ complex, these complexes interact differently with the interface.

The ^{51}V signal is significantly broadened upon placement of $[VO_2(ma)_2]^-$ in the CTAB reverse-micellar environment. The signal linewidth and chemical shifts of monoanionic $[VO_2(ma)_2]^-$ and $[VO_2(dipic)]^-$ complexes are compiled in Table 1. Increasing linewidth with decreasing w_0 is generally associated with restricted motions of the vanadium complex [35, 51, 70], caused by interaction with the interface and some degree of immobilization. Several other systems have been reported in which changes in the linewidths were found as w_0 decreased, such as V_{10} in AOT/isooctane RMs [51, 70] and $[VO_2(ma)_2]^-$ in AOT/isooctane [20]. These studies suggest that, in a large water pool, at least part of the complex is located in the water pool. When the water pool size (w_0) decreases, the complex is pushed nearer the interface and this is reflected in chemical shift changes. The observation of changes in the linewidth for $[VO_2(ma)_2]^-$ suggest that this compound is not nestled near the interface as was the case for $[VO_2(dipic)]^-$. Instead, part of the molecule is in the water pool and, as the w_0 size changes, its interaction with the surfactant layer also changes slightly.

The effect of the aqueous stock solution pH on the ^{1}H chemical shifts in $[VO_2(ma)_2]^-$ as a function of water pool size w_0 was studied at pH 7.0, 8.1, and 9.7 (Fig. 7). When compared with aqueous stock solution, an upfield shift is observed in most cases with decreasing w_0. Both protons are shifted upfield, although the C_{Hb} proton is most affected by changes in the water pool size. A smaller upfield shift is observed for C_{Ha}. This is consistent with a definite but modest effect and suggests that environment changes with changes in w_0 result from the coordinated complex interaction with the interface. Decreasing w_0 has almost no effect on the C_{CH_3} resonance, suggesting that this proton's environment remains similar regardless of the water pool size. These observations suggest that the methyl

Table 1 The ^{51}V NMR chemical shift and linewidth for $[VO_2(ma)_2]^-$ (where ma is maltol) and $[VO_2(dipic)]^-$ complexes in aqueous stock solutions (*Aq*) and micellar (*M*), and reverse-micellar (*RM*) systems

System	Probe	pH	Surfactant	Cosurfactant	w_0	$\delta(^{51}V)$ (ppm)	Linewidth (Hz)	Reference
Aq	$[VO_2(ma)_2]^-$	8.6	–	–	–	−496.9	486 ± 8	This work
Aq	$[VO_2(ma)_2]^-$	7.6	–	–	–	−495.6	420 ± 3	[20]
M	$[VO_2(ma)_2]^-$	7.3	10 mM CTAB	–	–	−491	1,400 ± 100	This work
M	$[VO_2(ma)_2]^-$	7.3	50 mM CTAB	–	–	−492	1,500 ± 150	This work
RM	$[VO_2(ma)_2]^-$	–	AOT	–	20	−495.2	630 ± 6	[20]
RM	$[VO_2(dipic)]^-$	–	CTAB	Amyl alcohol	20	−529.8	1,160 ± 30	[35]
RM	$[VO_2(ma)_2]^-$	–	0.1 M CTAB	0.5 M 1-pentanol	20	−493.7	1,080 ± 40	This work
RM	$[VO_2(ma)_2]^-$	–	0.1 M CTAB	0.5 M 1-pentanol	10	−496	2,300 ± 300	This work

CTAB cetyltrimethylammonium bromide, *AOT* sodium bis(2-ethylhexyl)sulfosuccinate (also abbreviated Aerosol-OT), *ma* maltolato

group is at the RM borderline of polar and nonpolar regions, that C_{Ha} is slightly penetrating the interface, and that C_{Hb} is deeper in the interface. However, the fact that changes are observed as w_0 varies suggests that parts of the complex are in the aqueous phase. If the complex is to be associated with both the interface and the water pool, that complex may have one ligand in the interface and another one in the water pool. Given the dynamic nature of this system, the molecule may be sampling two different environments on the NMR timescale; the NMR signal will average and result in observation of only one set of signals.

Interaction of maltol ligand with CTAB/1-pentanol/cyclohexane/D_2O RMs

The study with the free ligand is important in determining effects at the interface of the ligand alone and in a complex. This is particularly important for the $[VO_2(ma)_2]^-$ complex because it decomposes into free ligand and vanadate species in aqueous solution over the pH range studied. In contrast to the $[VO_2(ma)_2]^-$ complex, the maltol chemical shifts are pH-sensitive because of maltol deprotonation above neutral pH (pK_a 8.5 [53]) and result in an upfield shift of the signals with increasing pH of the aqueous stock solution (see below; Fig. S1, Table S2). Specifically, the L_{CH_3} proton shifts upfield by 0.08 ppm, L_{Ha} shifts upfield by 0.14 ppm, and L_{Hb} shifts upfield by 0.19 ppm upon maltol deprotonation from pH 5.1 to the monoanion (ma^-) at pH 10.8. These shifts serve as controls for comparison with the shifts of free maltol in CTAB/1-pentanol/cyclohexane RMs.

The maltol stock solutions at pH 7.0, 8.2, and 9.7 were combined with CTAB, 1-pentanol, and cyclohexane (0.2 M CTAB and 1.0 M 1-pentanol) to form clear and translucent solutions containing RMs of differing w_0. The formation of RMs in solutions with $w_0 = 12$ of approximately 6 nm size was confirmed using DLS and corresponded to formation of RMs reported in the literature [40]. The ^{1}H NMR chemical shifts for RM are shown in Fig. 7b as a function of w_0 and are compared with those in aqueous solution. The L_{CH_3} signal shifts upfield at pH 7.0 and 8.2, suggesting that ligand deprotonation and/or penetration of the interface takes place. At pH 9.7, however, both downfield and upfield shifts are observed depending on w_0, suggesting that methyl protons in deprotonated ma^- move from the more polar Stern layer into a less polar surfactant environment. Transition from upfield to downfield shifts with decreasing water pool size is also observed for L_{Ha} protons at pH 7.0. At pH 8.2 and 9.7, L_{Ha} is shifted downfield, suggesting that L_{Ha} is located in the polar Stern layer. Surprisingly, L_{Hb} is shifted upfield at all pH values, indicating penetration of the nonpolar region regardless of protonation state. Since there are differences in the chemical shifts of the maltol protons as w_0 changes, molecule orientation is sensitive to the RM water pool size.

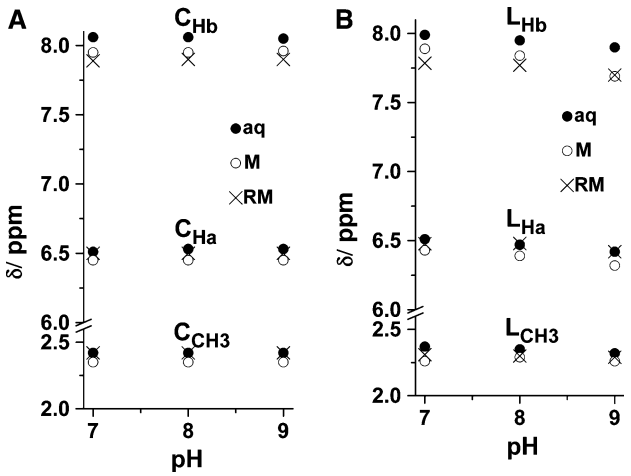

Fig. 8 The ^{1}H NMR chemical shifts of Hb, Ha, and CH_3 protons of the $[VO_2(ma)_2]^-$ complex (C_{Hb}, C_{Ha}, and C_{CH_3}) (**a**) and maltol ligand (L_{Hb}, L_{Ha}, and L_{CH_3}) (**b**) as a function of aqueous stock solution pH. The proton chemical shifts in aqueous stock solutions (*filled circles*), the 50 mM CTAB micelles (*open circles*), and the 0.2 M CTAB/1.0 M 1-pentanol/cyclohexane $w_0 = 4$ reverse-micelles (*crosses*) are compared

In Fig. 8 we compare the effects of complex versus free ligand, micelles, and RMs with aqueous stock solution as a function of pH. The reverse-micellar systems that we have used for comparison have $w_0 = 4$ because, for these small RMs, the differences in proton chemical shifts are greatest. Very similar chemical shifts are observed when the complex or only ligand is present. The Hb proton is affected most in the ligand at high pH. Otherwise the effects are small, as would be expected in the absence of deprotonation and if there is averaging of shifts from one ligand in the water pool and the other at the interface.

The effects of the complex and the ligand on the micelles and on the RMs were also similar. This is somewhat surprising because in the RMs the complex and the ligand are near the interface because of the size of the water pool, whereas in micelles the complex and the ligand can readily distribute in the aqueous phase. Given that the CTAB aggregation number is approximately 100, and assuming that the complex does not alter CTAB micelle formation in a solution of 2.0 mM $[VO_2(ma)_2]^-$ and 50 mM CTAB, there are approximately four $[VO_2(ma)_2]^-$ per CTAB micelle. The conductivity studies confirm that complex does not alter micelle formation (Fig. 5). In a reverse-micellar solution the micellar structure disruption is also unlikely; DLS results did not show any differences in the presence of the complex. We estimate that there are approximately two probe molecules per RM for $w_0 = 20$, and one probe per three RMs for $w_0 = 4$. Thus, the similar changes in chemical shifts in these two systems suggest that the location of the complex in the two systems is similar and is dictated by the degree of hydrophobicity in the environment and the nature of the complex/ligand.

On the basis of the data obtained with both the micellar system and the reverse-micellar system, the location of the complex and the maltol ligand can be proposed. As shown in Fig. 9a and b, we propose that both the complex and the ligand partially intercalate into the interface and are at an angle to properly account for the differential shifting of the Ha and Hb protons. The complex is shown with one ligand penetrating the surface as expected for a compound that has strong interactions with the interface but only modest chemical shift changes. The complex and ligand interact with the interface in the RMs in a similar manner as shown in Fig. 9c and d, although the presence of the cosurfactant 1-pentanol changes the nature of the interface. The complex in both these systems is partially penetrating, with the second ligand protruding into the water pool. This location is consistent with the observed chemical shift differences and the differential interaction with the water pool depending on the w_0 values. Although in the micellar system the complex and the ligand have the opportunity to remain in the aqueous phase, they are associated with the interface.

An interesting aspect of these studies is the observation that the $[VO_2(ma)_2]^-$ complex hydrolyzes in the presence

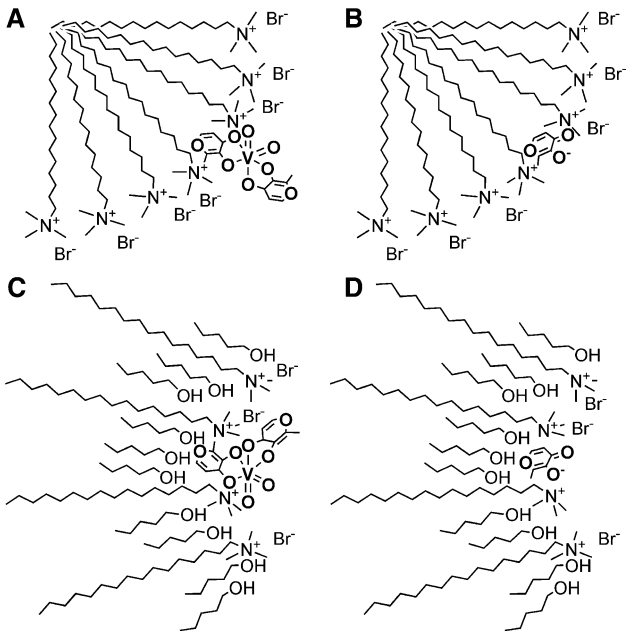

Fig. 9 Proposed location of the $[VO_2(ma)_2]^-$ complex (**a**, **c**) and the ma^- ligand (**b**, **d**) on the CTAB micellar (**a**, **b**) and reverse-micellar (**c**, **d**) interface. The $[VO_2(ma)_2]^-$ complex charge is omitted for clarity

of the interface. This is observed in the studies using either micelles and RMs. Solution stability of coordination complexes such as $[VO_2(ma)_2]^-$ [2, 13, 53] is dependent not only on pH, as demonstrated, but also on ionic strength, solvent hydrophobicity, and temperature. Other components in solution also play an important role. These factors could therefore contribute to the observation that the coordination complex is hydrolyzing in the presence of the interface. Pharmacokinetic studies have demonstrated that the BMOV complex falls apart in vivo following administration [71, 72]. Although the question of when hydrolysis takes place has not specifically been determined, these studies have demonstrated that the ligand and the metal will, nonetheless, separate in a biological system. Since the vanadium is generally believed to be transported by transferrin [73, 74], the hydrolysis would take place prior to the complex reaching the bloodstream. These studies provide evidence that the oxidized BMOV molecule will hydrolyze in the presence of an ionic interface. Since $[VO_2(ma)_2]^-$ is a known oxidation product of BMOV, combined these studies provide experimental support for the notion that the ligand of BMOV (maltol) will dissociate from the metal upon administration in animals [71, 72].

Conclusions

In this study we have identified the effects of the CTAB micellar and reverse-micellar interface on the antidiabetic

vanadium(V) complex $[VO_2(ma)_2]^-$ and its dissociation product maltol. We used both ^1H and ^{51}V NMR spectroscopy to monitor events near the interface, utilizing chemical shifts to probe the location and/or deprotonation and the signal linewidth to evaluate probe association with the interface. Our data suggest that the location of the $[VO_2(ma)_2]^-$ probe in the interface is similar in both micelles and RMs. However, the interface charge, water pool size, and surface curvature contribute to the probe penetration and its hydrolytic stability. The CTAB micelle formation above the cmc and reduction of water pool size in the RMs facilitated the $[VO_2(ma)_2]^-$ decomposition into vanadium(V) species and free maltol ligand. ^1H NMR measurements of free maltol ligand are affected by maltol ligand deprotonation. Thus, both molecule location and protonation have to be considered. We conclude that the positively charged CTAB interface in micelles and RMs facilitates the expected maltol deprotonation into ma^- and H^+. Line broadening in micellar and reverse-micellar solutions and comparison with ^1H chemical shifts in aqueous solutions without surfactant also suggest that maltol is penetrating the interface, most likely as the monoanion. The maltol location in the interface is pH-sensitive, and does change with the water pool size variation in the reverse-micellar solution. Together, our results provide details on how the oxidized BMOV complex, $[VO_2(ma)_2]^-$, may interact in vivo with biological membranes. Reducing the water pool size facilitates the $[VO_2(ma)_2]^-$ complex decomposition, suggesting that similar processes may take place under conditions of limited hydration near the cell plasma membrane or membranes of intracellular organelles.

These findings are also important for understanding the antidiabetic activity of vanadium compounds such as BMOV. The stability of BMOV's oxidized metabolite $[VO_2(ma)_2]^-$ near the CTAB interface suggests that the biologically active species may be a partially dissociated complex or ligand-free aqueous vanadium(V) species. However, the environment of the ligand, the charge of the vanadium species, and complex hydrophobicity are also critically important for interaction with the membrane.

Acknowledgments D.C.C. and D.A.R. thank the National Science Foundation (0628260, CRC) for funding. We also thank Chris D. Rithner and the Department of Chemistry's Central Instrument Facility for technical assistance.

References

1. Thompson KH, Lichter J, LeBel C, Scaife MC, McNeill JH, Orvig C (2009) J Inorg Biochem 103:554–558
2. Crans DC, Smee JJ, Gaidamauskas E, Yang L (2004) Chem Rev 104:849–902
3. Thompson KH (1999) Biofactors 10:43–51
4. Rehder D (2003) Inorg Chem Commun 6:604–617
5. Barrio DA, Etcheverry SB (2010) Curr Med Chem 17:3632–3642
6. McLauchlan CC, Hooker JD, Jones MA, Dymon Z, Backhus EA, Youkhana MA, Manus LM (2010) J Inorg Biochem 104:274–281
7. Li M, Smee JJ, Ding W, Crans DC (2009) J Inorg Biochem 103:585–589
8. Gao XL, Lu LP, Zhu ML, Yuan CX, Ma JF, Fu XQ (2009) Acta Chim Sin 67:929–936
9. Yuan CX, Lu LP, Gao XL, Wu YB, Guo ML, Li Y, Fu XQ, Zhu ML (2009) J Biol Inorg Chem 14:841–851
10. Roess DA, Smith SML, Winter P, Zhou J, Dou P, Baruah B, Trujillo AM, Levinger NE, Yang X, Barisas BG, Crans DC (2008) Chem Biodivers 5:1558–1570
11. Sakurai H (2008) J Pharm Soc Jpn 128:317–322
12. Sakurai H, Yoshikawa Y, Yasui H (2008) Chem Soc Rev 37:2383–2392
13. Rehder D, Pessoa JC, Geraldes CFGC, Castro MMCA, Kabanos T, Kiss T, Meier B, Micera G, Pettersson L, Rangel M, Salifoglou A, Turel I, Wang DR (2002) J Biol Inorg Chem 7:384–396
14. Yang XG, Wang K, Lu JF, Crans DC (2003) Coord Chem Rev 237:103–111
15. Yang XG, Yang XD, Yuan L, Wang K, Crans DC (2004) Pharm Res 21:1026–1033
16. Faneca H, Figueiredo VA, Tomaz I, Goncalves G, Avecilla F, de Lima MCP, Geraldes CFGC, Pessoa JC, Castro MMCA (2009) J Inorg Biochem 103:601–608
17. Xie MJ, Niu YF, Yang XD, Liu WP, Li L, Gao LH, Yan SP, Meng ZH (2010) Eur J Med Chem 45:6077–6084
18. Islam MN, Kumbhar AA, Kumbhar AS, Zeller M, Butcher RJ, Dusane MB, Joshi BN (2010) Inorg Chem 49:8237–8246
19. Hiromura M, Nakayama A, Adachi Y, Doi M, Sakurai H (2007) J Biol Inorg Chem 12:1275–1287
20. Aureliano M, Henao F, Tiago T, Duarte RO, Moura JJG, Baruah B, Crans DC (2008) Inorg Chem 47:5677–5684
21. Winter PW, Al-Qatati A, Wolf-Ringwall AL, Schoeberl S, Crans DC, Van Orden AK, Barisas BG, Roess DA (2011) (submitted)
22. Gupta S, Moulik SP (2008) J Pharm Sci 97:22–45
23. Lawrence MJ, Rees GD (2000) Adv Drug Deliv Rev 45:89–121
24. Langevin D (1992) Annu Rev Phys Chem 43:341–369
25. Chevalier Y, Zemb T (1990) Rep Prog Phys 53:279–371
26. Fendler JH (1987) Chem Rev 87:877–899
27. Choi SY, Oh SG, Lee JS (2001) Coll Surf B 20:239–244
28. Kreke PJ, Magid LJ, Gee JC (1996) Langmuir 12:699–705
29. Vermathen M, Stiles P, Bachofer SJ, Simonis U (2002) Langmuir 18:1030–1042
30. Gaidamauskas E, Cleaver DP, Chatterjee PB, Crans DC (2010) Langmuir 26:13153–13161
31. Correa NM, Biasutti MA, Silber JJ (1995) J Colloid Interface Sci 172:71–76
32. Falcone RD, Correa NM, Biasutti MA, Silber JJ (2000) Langmuir 16:3070–3076
33. Rack JJ, McCleskey TM, Birnbaum ER (2002) J Phys Chem B 106:632–636
34. Aureliano M, Crans DC (2009) J Inorg Biochem 103:536–546
35. Stover J, Rithner CD, Inafuku RA, Crans DC, Levinger NE (2005) Langmuir 21:6250–6258
36. Crans DC, Rithner CD, Baruah B, Gourley BL, Levinger NE (2006) J Am Chem Soc 128:4437–4445
37. Goyal PS, Aswal VK (2001) Curr Sci India 80:972–979
38. Palazzo G, Carbone L, Colafemmina G, Angelico R, Ceglie A, Giustini M (2004) Phys Chem Chem Phys 6:1423–1429
39. Palazzo G, Lopez F, Giustini M, Colafemmina G, Ceglie A (2003) J Phys Chem B 107:1924–1931
40. Giustini M, Palazzo G, Colafemmina G, DellaMonica M, Giomini M, Ceglie A (1996) J Phys Chem 100:3190–3198

41. Li F, Li GZ, Wang HQ, Xue QJ (1997) Colloids Surf A 127:89–96
42. Grieser F, Drummond CJ (1988) J Phys Chem 92:5580–5593
43. Song AM, Zhang JH, Zhang MH, Shen T, Tang JA (2000) Colloids Surf A 167:253–262
44. Biswas S, Bhattacharya SC, Sen PK, Moulik SP (1999) J Photochem Photobiol A 123:121–128
45. Mchedlov-Petrossyan NO, Vodolazkaya NA, Gurina YA, Sun WC, Gee KR (2010) J Phys Chem B 114:4551–4564
46. Alargova RG, Danov KD, Petkov JT, Kralchevsky PA, Broze G, Mehreteab A (1997) Langmuir 13:5544–5551
47. May S, Ben-Shaul A (2001) J Phys Chem B 105:630–640
48. Angelico R, Palazzo G, Colafemmina G, Cirkel PA, Giustini M, Ceglie A (1998) J Phys Chem B 102:2883–2889
49. Yuen VG, Orvig C, McNeill JH (1997) Am J Physiol Endocrinol Metab 35:E30–E35
50. Yuen VG, Caravan P, Gelmini L, Glover N, McNeill JH, Setyawati IA, Zhou Y, Orvig C (1997) J Inorg Biochem 68:109–116
51. Crans DC, Trujillo AM, Bonetti S, Rithner CD, Baruah B, Levinger NE (2008) J Org Chem 73:9633–9640
52. Castro MMCA, Geraldes CFGC, Gameiro P, Pereira E, Castro B, Rangel M (2000) J Inorg Biochem 80:177–179
53. Caravan P, Gemini L, Glover N, Herring FG, Li H, McNeill JH, Rettig SJ, Setyawati IA, Shuter E, Sun Y, Tracey AS, Yuen VG, Orvig C (1995) J Am Chem Soc 117:12759–12770
54. Ekwall P, Mandell L, Fontell K (1969) J Colloid Interface Sci 29:639–646
55. Rodenas E, Valiente M (1992) Colloids Surf 62:289–295
56. Vautier-Giongo C, Bales BL (2003) J Phys Chem B 107:5398–5403
57. Harris RK, Becker ED, De Menezes SMC, Granger P, Hoffman RE, Zilm KW (2008) Pure Appl Chem 80:59–84
58. Modaressi A, Sifaoui H, Grzesiak B, Solimando R, Domanska U, Rogalski M (2007) Colloids Surf A 296:104–108
59. Pettersson L, Andersson I, Hedman B (1985) Chem Scr 25:309–317
60. Pettersson L, Hedman B, Andersson I, Ingri N (1983) Chem Scr 22:254–264
61. Pettersson L, Andersson I, Gorzsas A (2003) Coord Chem Rev 237:77–87
62. Crans DC, Rithner CD, Theisen LA (1990) J Am Chem Soc 112:2901–2908
63. Saponja JA, Vogel HJ (1996) J Inorg Biochem 62:253–270
64. Crans DC, Baruah B, Ross A, Levinger NE (2009) Coord Chem Rev 253:2178–2185
65. Wittenkeller L, Abraha A, Ramasamy R, Defreitas DM, Theisen LA, Crans DC (1991) J Am Chem Soc 113:7872–7881
66. Rico I, Lattes A (1986) J Phys Chem 90:5870–5872
67. Treiner C, Makayssi A (1992) Langmuir 8:794–800
68. Szakacs Z, Kraszni M, Noszal B (2004) Anal Bioanal Chem 378:1428–1448
69. Elvingson K, Baro AG, Pettersson L (1996) Inorg Chem 35:3388–3393
70. Baruah B, Roden J, Sedgwick M, Correa MN, Crans DC, Levinger NE (2006) J Am Chem Soc 128:12758–12765
71. Setyawati IA, Thompson KH, Yuen VG, Sun Y, Battell M, Lyster DM, Vo C, Ruth TJ, Zeisler S, McNeill JH, Orvig C (1998) J Appl Physiol 84:569–575
72. Thompson KH, Liboiron BD, Bellman YSKDD, Setyawati IA, Patrick BO, Karunaratne V, Rawji G, Wheeler J, Sutton K, Bhanot S, Cassidy C, McNeill JH, Yuen VG, Orvig C (2003) J Biol Inorg Chem 8:66–74
73. Kiss T, Jakusch T, Hollender D, Dornyei A, Enyedy EA, Pessoa JC, Sakurai H, Sanz-Medel A (2008) Coord Chem Rev 252:1153–1162
74. Pessoa JC, Tomaz I (2010) Curr Med Chem 17:3701–3738